Effects of Temperature on Early Crack Formation in Portland Cement Concrete Pavements

YEOU-SHANG JENQ, CHWEN-JANG LIAW, AND SANG-CHEL KIM

Major distress problems of concrete pavements generally start with crack formation caused by the combined effects of traffic load and service temperature. Water and salt can easily infiltrate into pavement at the location of cracks and create durability and structural problems. Although crack formation has an important effect on the durability and structural capacity of concrete pavements, studies on the crack formation mechanisms in concrete are still limited to conventional stress-based or strain-based elasticity analysis because of the complexity of the problem. Recently because of the promising features of fracture mechanics–based models, fracture mechanics analysis on concrete structures is receiving more attention from researchers. A cohesive crack model was used to study the effect of temperature on crack formation in concrete pavements and to demonstrate the feasibility of fracture mechanics analysis on concrete pavement systems. It was found that the peak temperature differential that causes formation of random cracks in the pavement is sensitive to the age of the pavement; to properly control the occurrence of random cracking, saw-cut grooves should be introduced at the earliest possible age of the concrete pavement.

Major distress problems of concrete pavements generally start with crack formation caused by the combined effects of traffic load and service temperature. Water and salt can easily infiltrate into the pavement at the location of cracks and create durability and structural problems. Crack formation in concrete pavements can be a progressive development caused by, for example, traffic-induced fatigue or even a single-occurrence overloaded truck or thermal stress resulting from a large temperature change. Although crack formation has an important effect on the durability and structural capacity of concrete pavements, studies on the crack formation mechanisms in concrete pavements are still limited to the conventional stress-based or strain-based elasticity analysis. It has been shown that conventional models are not able to capture some widely observed size effect and notch sensitivity behavior on concrete structures and that models developed on the basis of fracture mechanics theories are more suitable for describing crack development in concrete materials (*1*). Because of the promising features of fracture mechanics-based models, the application of these models to analyzing actual concrete structures is receiving more attention from researchers. One of the advantages of using the fracture mechanics-based models is that the extrapolation capability of these models is much better than that of conventional models in terms of dynamic loading conditions and various geometrical configurations of the concrete structures.

In the present paper, the effects of temperature on the crack formation mechanisms caused by an artificially introduced groove are analyzed to demonstrate the feasibility of fracture mechanics analysis on concrete pavement systems. A saw-cut groove is generally introduced to confine crack formation at the location of the groove at a controlled spacing—for example, 3.66 m (12 ft). A better design for the optimum groove depth calls for better understanding of how the artificially introduced groove affects crack formation in the pavement.

Department of Civil Engineering, The Ohio State University, Columbus, Ohio 43210.

COHESIVE CRACK MODEL

In modeling crack formation and crack propagation in concrete, a crack can generally be modeled as a Griffith-type traction-free cracks (*2*) or a Dugdale-Barenblatt type of cohesive crack (*3–6*). In this paper, the cohesive crack concept proposed by Hillerborg et al. (*5*) will be used. The cohesive crack concept assumes that when a crack starts to develop in a material, this crack is still able to transfer some forces. The crack zone that is bridged by this cohesive force, which is generally termed the "process zone" (see Figure 1), is governed by the applied load, structure and sample geometries, and the basic properties of the material. The cohesive crack concept was originally proposed by Dugdale (*3*) and Barenblatt (*4*) for metals and by Hillerborg et al. (*5*) for portland cement concrete (PCC) to characterize progressive crack development in these materials.

Several assumptions were made in the cohesive crack model (*5*):

1. The process zone is assumed to initiate when the first principal stress reaches the tensile strength (f_t, as defined in Figure 2*a* and *b*).
2. The direction of the process zone will be perpendicular to the direction of the first principal stress.
3. The properties of the materials outside the process zone are governed by a stress-strain relationship (Figure 2*a*). The stress-strain curve does not have to be linear. However, for simplicity, a linear relationship can be assumed.
4. The material in the process zone is able to transfer stress, and the stress-transferring capability depends on its opening displacement according to the stress-separation relationship shown in Figure 2*b*.

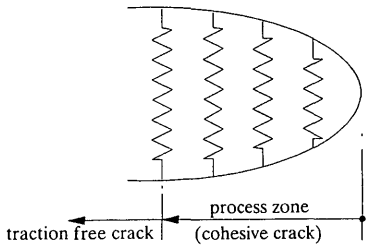

FIGURE 1 Cohesive crack modeled by nonlinear spring.

On the basis of these assumptions, the size of the process zone, the magnitude of the bridging stress, and the applied load can be determined (*5,6*). The proposed stress-separation curve concept is the key factor that separates the proposed fracture mechanics model from the conventional strain-based or stress-based models. Since strain cannot be defined objectively when there are displacement discontinuities (e.g., a crack), a fracture mechanics model is more suitable in characterizing the fracture mechanisms in a material.

NUMERICAL FORMULATION

For simplicity, a notched beam is used to demonstrate the numerical formulation for the proposed cohesive crack model. Consider a notched beam with a preexisting crack up to Node n subjected to a load P in the midspan, as indicated in Figure 3 (top). It was assumed that the process zone would develop along a straight plane, which is reasonable for Mode I crack propagation. When the beam is loaded, by introducing the closing stresses over the crack, one can analyze the progressive crack development in the beam.

In the calculation process, the stresses acting across a cohesive crack are replaced by equivalent nodal forces. These forces can be determined according to the stress-separation curve when the width at the cohesive crack zone is known. As indicated in Figure 3 (top), when the first node reaches its tensile strength, the opening displacement at the first node is still equal to zero, that is, $\sigma_1 = f_t$, $w_1 = \ldots = w_{n-1} = 0$. From this, one can determine the first point, which corresponds to the crack initiation point, of the load-load line

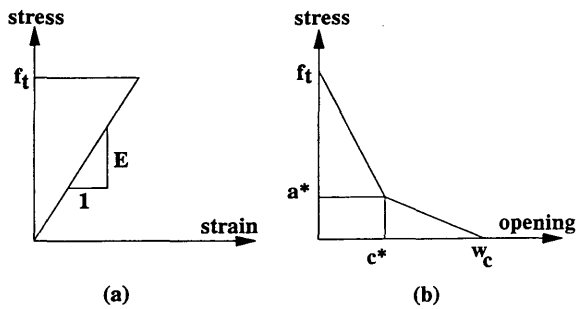

FIGURE 2 (*a*) Deformation properties of the material outside the fracture zone can be obtained from a σ-ε curve; (*b*) those of the fracture zone can be obtained from a σ-*w* curve.

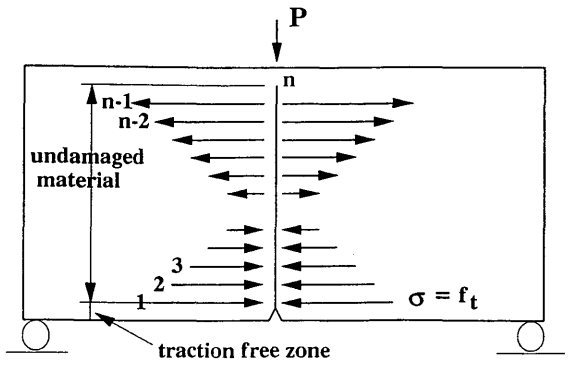

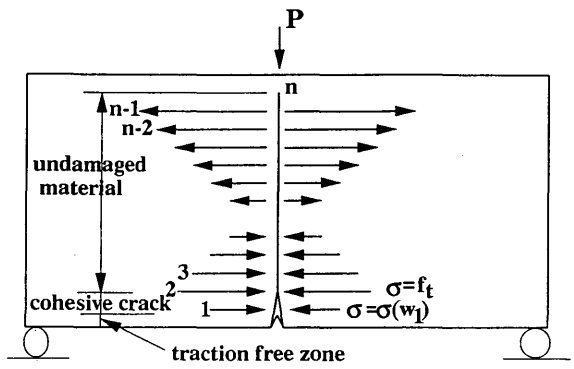

FIGURE 3 Notched beam subjected to three-point bending: *top*, at crack initiation; *bottom*, schematic illustration of the second step.

deflection ($P - \delta$) curve and the load-crack mouth opening displacement (P-CMOD) curve.

When the crack starts to propagate as shown in Figure 3 (bottom), the first node is opened and the second node is assumed to reach the tensile strength. At this point the boundary conditions can be expressed as $\sigma_2 = f_t$, $w_2 = w_3 = \ldots = w_{n-1} = 0$, $w_1 \neq 0$, and $\sigma_1 = \sigma(w_1)$. The system of equations is nonlinear because of the stress-separation constraint. Therefore, an iteration process is needed for this step.

Following the same principle, the progress of the crack propagation can be analyzed, and complete $P - \delta$ and $P -$ CMOD curves can be generated. The driving force for crack propagation in a pavement system is not limited to the applied load (P). Service temperature differential (T), which is defined as the temperature difference from the surface to a certain depth of the pavement, can also be the driving force for crack propagation. The principle involved in the numerical formulation, however, is the same for the applied load and service temperature. Thus, one can derive the numerical formulation for temperature loading by replacing the effect of applied load with that of temperature. To obtain the theoretical results using the proposed cohesive crack model, a numerical method such as a finite element method must be applied.

CRACK CONTROL

Under ideal conditions a pavement slab will respond to temperature differentials across its thickness as follows. Assuming

no-curl (flat) condition at the reference temperature, a negative temperature differential—which means that the surface temperature is lower than the temperature at the bottom slab—makes the slab curl upward at the edges, with the corners exhibiting the greatest curling, whereas the center stays in contact with the subgrade. In contrast, a positive temperature differential causes reverse results. Thus, a high thermal tensile stress will occur at the center of the slab at negative temperature differential, whereas a high thermal compressive stress may occur at the center at positive temperature differential. In either case, part of the concrete slab is not in direct contact with the subbase, and bending action caused by the applied traffic load can further increase the magnitude of tensile stresses in the pavement. Since concrete has a very low tensile strength compared with its compressive strength, a combined tensile stress induced by temperature gradient and traffic loads can easily crack the pavement. Furthermore, for a long concrete slab, formation of these cracks can occur randomly.

To control random cracking in plain concrete pavements, current practice requires the introduction of a saw-cut groove of about one-third or one-fourth of the concrete pavement thickness when the pavement is about 1 to 3 days old. After the groove is introduced and before the pavement is open to traffic, a natural crack may or may not develop at the location of the groove, depending on the magnitude of the thermal stress caused by temperature change and the concrete's properties. Adequate groove depth must be provided to ensure that the transverse cracks will be confined at the location of the groove. If the groove is not deep enough, cracks may form outside the groove (*7*), which will cause costly maintenance and repair work later. However, a groove depth that is too deep may not be economical, because it will require more work during the cutting and sealing processes. The adequacy of the groove depth is also highly dependent on the age of the concrete pavements; in some cases timing of the cut is more important than the depth of the cut in terms of crack control, especially if a high shrinkage deformation is expected at a very early concrete pavement age.

To better understand factors affecting crack formation in grooved (or notched) concrete pavements, a parametric study was performed and an experimental program was designed to evaluate the material properties needed for the theoretical model.

EXPERIMENTAL PROGRAM

Because the artificial groove generally is introduced to the pavements within 3 days after placement of concrete, it is important to evaluate the concrete fracture properties at an early age. The fracture parameters evaluated are the tensile strength, the fracture energy, and the shape of the stress-separation curve. An experimental program was designed to assess these fracture properties at various ages. Determination of these parameters is discussed in the following section.

Preparation of Concrete Specimen

Sand and pea gravel with maximum aggregate size of 0.95 cm (⅜ in.) were used to fabricate the concrete samples. All the aggregates were dried in the oven for 24 hr and then exposed to air at room temperature to maintain a constant water content in the aggregates. The mix proportion for cement, sand, pea gravel, and water was 1.0:2.6:2.6:0.5, which was used by Jenq and Shah (*2*). Beam specimens and cylinder specimens were prepared for the study. The beams were used for three-point bending tests and indirect tensile tests, whereas the cylinders were for compressive tests. Some of the beams were saw-cut with a notch-depth ratio of 1:3. The dimensions of the beam specimen were 30.48 cm (12 in.) long, 7.62 cm (3 in.) high, and 2.54 cm (1 in.) thick. The dimensions of the cylinder specimen were 7.62 cm (3 in.) in diameter and 15.24 cm (6 in.) high. Specimens were tested at 16 hr, 1 day, 3 days, 7 days, 14 days, and 28 days. Each series consisted of 11 samples, which included four notched beams, four unnotched beams, and three cylinders.

Three-Point Bending Tests

Notched beam tests and unnotched beam tests were conducted using three-point bending tests. During the test, the applied load, the CMOD, and the load-point deflection (δ) were monitored and stored in a digital form. The rate of loading was controlled by a constant increment of CMOD. Various loading rates for notched beams were applied, with a range of 0.46 to 0.66 mm/min (0.018 to 0.026 in./min) depending on the ages, whereas a constant loading rate of 0.25 mm/min (0.01 in./min) was given for unnotched beams. Typical load-load line deflection and load-CMOD curves obtained from the test are given in Figure 4. From these two curves, Young's modulus, fracture energy (G_f), and shape of the stress-separation curve can be evaluated.

Indirect Tensile Tests

To calculate the tensile strength, splitting tensile tests were conducted by loading one-half of the broken beam tested in the three-point bend tests. The test was performed under displacement control (load-line deflection control). The loading rate was fixed at 0.25 mm/min for all ages of concrete.

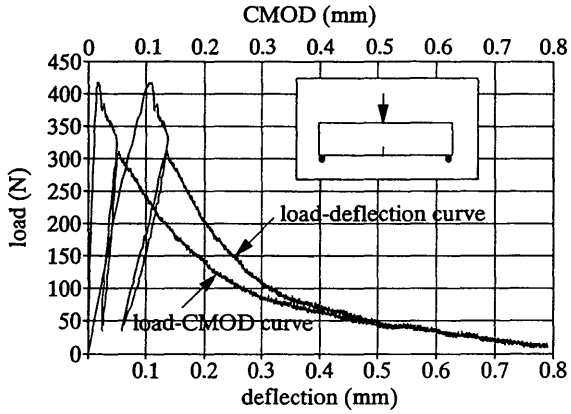

FIGURE 4 Typical load-load line deflection and load-CMOD curves.

TABLE 1 Material Properties of Concrete Obtained from Experiments

Age	16-hrs	1-day	3-days	7-days	14-days	28-days
Young's modulus, E (GPa)						
- from load-CMOD curve	8.34	14.69	21.03	25.45	26.90	30.28
- from load-deflection curve	6.21	8.97	20.01	22.07	24.14	26.90
Fracture energy, G_f (N/m)	10.16	30.13	52.21	44.68	61.85	85.85
Indirect tensile strength, f_t (MPa)	0.33	0.88	1.32	1.63	1.57	2.06
Modified tensile strength, f_t (Mpa)	0.58	1.44	2.40	2.86	3.65	3.81
Poisson's ratio, ν	0.2	0.2	0.2	0.2	0.2	0.2
Coefficient of thermal expansion, k (10^{-6}/°C)	3.09	3.09	3.09	3.09	3.09	3.09

1 GPa=0.1450x106 psi, 1 MPa=145 psi, 1 N=0.225 lb, 1 N/m=0.00571 lb/in, 1/°C=1.8/°F

EXPERIMENTAL RESULTS

Material parameters of concrete evaluated at various ages from the tests are summarized in Table 1. As expected, Young's modulus increases with the age of the concrete. However, the Young's modulus values calculated from the load-CMOD curves are higher than those obtained from the load-deflection curves. Lower modulus values obtained from the load-deflection curves may be caused by additional settlement deflection at supporting points. Similar results were also reported by other researchers.

Fracture energy is defined as the area under the load-line deflection curve divided by the initial uncracked ligament area (*8*). Although the area under the load-CMOD curve does not have a direct physical meaning, the fracture energy calculated from the area under load-CMOD curves seems to be comparable with that obtained from load-deflection curves, as indicated in Figure 5. This suggests that the *P*-CMOD curve should be used to determine the fracture energy, since CMOD value is less sensitive to support settlements. Fracture energy was found to increase as the age of concrete increases.

Since the shape of a softening stress-separation curve also has a major influence on the calculated results, it is necessary to find a stress-separation curve that best describes (or fits) the material behavior. The shape of the stress-separation curve is dependent on the tensile strength (f_t), a^*, and c^*, as defined in Figure 2, provided that the fracture energy, which is the same as the area under the stress-separation curve, is kept constant. On the basis of the fracture energy and indirect tensile strength determined from the experimental program and assuming different values of a^* and c^*, theoretical predictions on the load-CMOD curves can be obtained. After a lengthy numerical experiment, it was concluded that the splitting tensile strength obtained from the beam samples was too low to yield a reasonable prediction. As a result, modified tensile strengths (see Table 1) along with various shape factors were used. Some theoretical *P*-CMOD curves were plotted in Figure 6 along with the experimental results for 16-hr-old concrete. On the basis of these numerical experiments, modified tensile strengths for concrete of various ages along with constant shape factors of $a^* = 0.25$ and $c^* = 0.1$ were used as the input material properties for the proposed model.

NUMERICAL ANALYSIS

Concrete pavements with various slab thicknesses and a known temperature distribution were analyzed. The thicknesses of

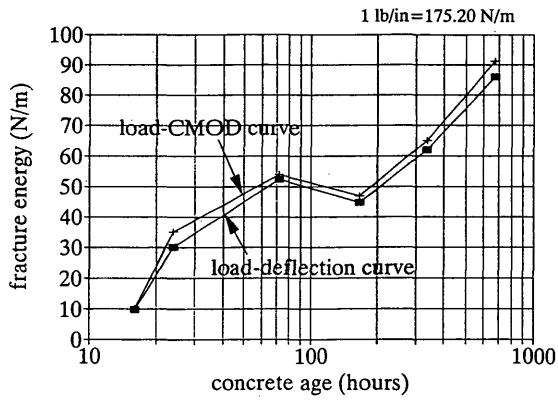

FIGURE 5 Fracture energy calculated from load-CMOD curve and load-deflection curve (notched beam).

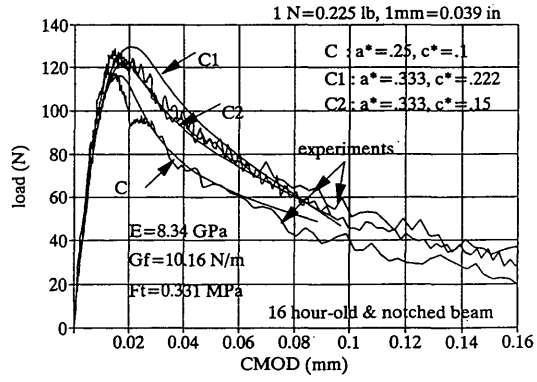

FIGURE 6 Experimental results and numerical results obtained from various combinations of a^* and c^* for 16-hr-old concrete.

the subbase and the subgrade are 22.86 cm (9 in.) and 203.2 cm (80 in.). The span of the slab is 7.32 m (24 ft). In this analysis, the material properties of concrete at 16 hr, 1 day, and 3 days were based on experimental results (Table 1). Young's modulus, Poisson's ratio, and coefficient of thermal expansion are 0.35 GPa (5.0×10^4 psi), 0.3, and 2.22×10^{-6}/°C (4.0×10^{-6}/°F) for subbase, and 0.21 GPa (3.0×10^4 psi), 0.4, and 2.0×10^{-6}/°C (3.6×10^{-6}/°F) for subgrade, respectively (*9*). For the present analysis, only temperature effect is considered, since no traffic load is expected for concrete pavements at this early age (i.e., less than 3 days old). Shrinkage deformation, which can be indirectly incorporated into the temperature analysis, is not explicitly considered in the present analysis.

The pavement system was analyzed in a three-layer system as indicated in Figure 7. Because of the symmetry of the pavement, only half of the slab was analyzed. It was also assumed that the subbase and subgrade (or soil) cannot resist any tensile stress, which is why free boundary conditions were prescribed on the left part of the pavement. The finite element mesh used in the analysis is given in Figure 8. A finer mesh was used at the location of crack formation for better numerical accuracy. ABAQUS finite element package was used in all the finite element analyses.

Because the driving force in the present study is temperature, temperature distribution in the pavement should be prescribed first. A parabolic equation was used to describe the temperature distribution along the depth of the pavement. This assumption was based on the results of field temperature measurement (*8,11*). A uniform temperature distribution below 38.1 cm (15 in.) of the pavement surface was also assumed. A typical unit temperature differential profile is given in Figure 9. The relative temperature difference below 38.1 cm (15 in.) deep was assumed to be zero. Knowing the temperature profile, the effects of temperature differential (T) on the crack formation in the pavement system can be evaluated. Stress analysis was first performed on the pavement system without any crack formation. It was found that the highest tensile stress occurred at the top of the midspan of the concrete pavement. Thus, it was assumed that a crack will initiate at the top of the midspan of the pavement and propagate downward to the subgrade.

On the basis of the same numerical formulation principle discussed earlier, the opening displacement of the crack at

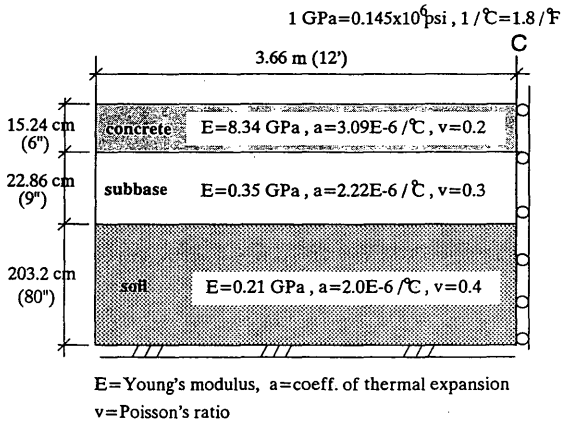

FIGURE 7 Boundary conditions.

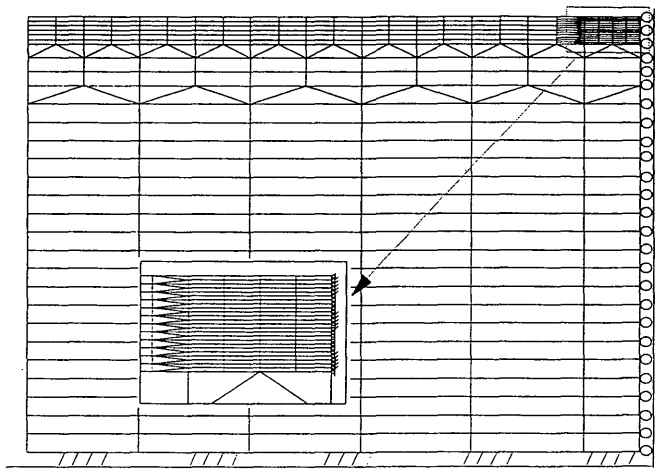

FIGURE 8 Finite element mesh.

each node and at the reference point can be calculated from the following equations:

$$w_i = \sum_{j=1}^{n-1} a_{ij}\sigma_j + c_j T \tag{1}$$

$$w_R = \sum_{j=1}^{n-1} b_j\sigma_j + d_T T \tag{2}$$

$$\begin{bmatrix} a_{11} & a_{12} & \cdots & a_{1(n-1)} & c_1 \\ a_{21} & a_{22} & \cdots & a_{2(n-1)} & c_2 \\ \cdots & \cdots & \cdots & \cdots & \cdots \\ a_{(n-1)1} & a_{(n-1)2} & \cdots & a_{(n-1)(n-1)} & c_{n-1} \\ b_1 & b_2 & \cdots & b_{n-1} & d_T \end{bmatrix} \times \begin{bmatrix} \sigma_1 \\ \sigma_2 \\ . \\ \sigma_{n-1} \\ T \end{bmatrix} = \begin{bmatrix} w_1 \\ w_2 \\ . \\ w_{n-1} \\ w_R \end{bmatrix} \tag{3}$$

or

$$\{C\}[\mathbf{F}] = [\Delta] \tag{4}$$

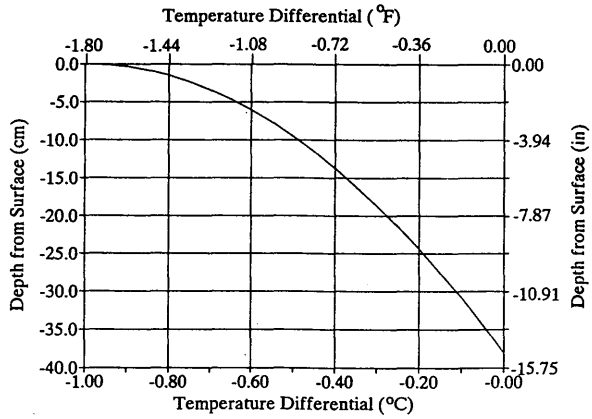

FIGURE 9 Unit parabolic temperature differential in concrete pavements.

where

a_{ij} = opening displacement of the crack at Node i when an equivalent closing force is acting at Node j,
c_j = opening displacement of the crack at Node i when a unit negative temperature differential is applied,
b_j = opening at the reference point when an equivalent closing force is acting at Node j,
d_T = opening at the reference point when a unit negative temperature differential is applied,
σ_j = closing pressure at Node j,
w_i = opening of the crack at Node i, and
w_R = opening of the reference point.

The square matrix, $\{C\}$, in Equation 4 is referred to as the influence matrix. In the influence matrix, except for the last column, the ith column represents the opening displacement at each node and at the reference point when a pair of equivalent unit closing forces acts at the ith node point. The reference point can be an arbitrary point that is of interest to the engineers. For example, for a three-bend point loading configuration, the load point can be chosen to be the reference point. The selection of the reference point, however, does not affect the numerical results. The last column represents the openings at each node and the opening at the reference point when a negative unit temperature differential is applied at the reference point. The vector [**F**] represents the closing pressure at each node and the applied temperature differential and the vector [**Δ**] represents the opening displacement at each node and the reference point.

Thus, on the basis of the calculation procedures discussed in earlier sections, a complete temperature differential versus CMOD curve and crack growth development due to temperature differential can be generated. The definition of CMOD used here is the same as that for the crack opening displacement at the top of the concrete slab.

DISCUSSION OF RESULTS

Figure 10 gives the development of crack formation with respect to the change of temperature differential. Each data point represents an element-length crack advancement in the concrete slab. Stable crack formation was first observed, because further crack advancement requires a higher temperature differential, as can be seen in Figure 10. However, when the peak temperature differential is reached, crack advancement becomes unstable (especially for an a/b ratio less than 0.25) because further crack propagation requires a lower temperature differential. Thus, when the peak temperature differential is reached, one can conclude that a through crack is formed in the concrete pavement. Figure 10 also indicates that the peak temperature differential decreases as the notch-depth ratio increases. Therefore, if the temperature differential in the field is lower than usual, a deeper groove is needed to ensure proper crack control. A value of $a/b = 0$ represents the temperature differential that may cause the formation of a random crack in the plain concrete pavement. For this particular case, this temperature differential is about 16.67°C (30°F) for a 16-hr-old pavement. This peak temperature will be even lower if the effect of shrinkage is included. If the expected temperature differential is higher than 16.67°C (30°F), then the groove (or cut) has to be introduced before the concrete is 16 hr old to prevent the occurrence of random cracking. Once random cracks form, the introduction of a saw-cut groove to control crack formation will not be very effective.

Effects of groove-depth ratio (or notch-depth ratio) and age on crack formation at various temperature differentials are given in Figures 11 and 12. As indicated, the thicker the concrete pavement, the lower is the groove-depth ratio (or notch-depth ratio) necessary for crack control. This also confirms the fact that concrete pavements also exhibit similar size-effect and notch sensitivity behavior (*1*), as observed in other types of concrete structures. Figures 11 and 12, however, reflect only the effect of groove-depth ratio. Timing is also critical for the overall final crack control; that is, the groove has to be introduced before random cracks occur, as discussed earlier. Thus, for better crack control, the groove should be introduced at the earliest allowable age without damaging the pavement.

On the basis of the proposed approach and with the knowledge of the expected temperature differential and the pave-

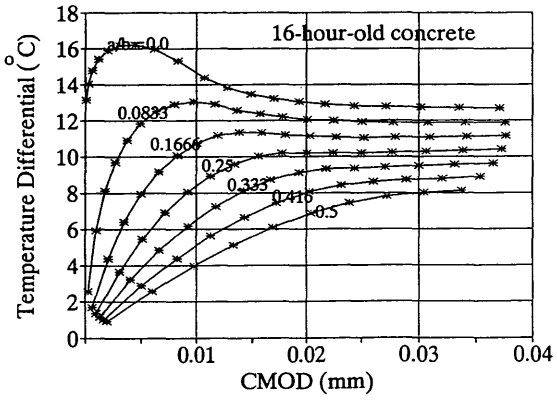

FIGURE 10 Development of temperature differential with various notch-depth ratios for 16-hr-old concrete pavement.

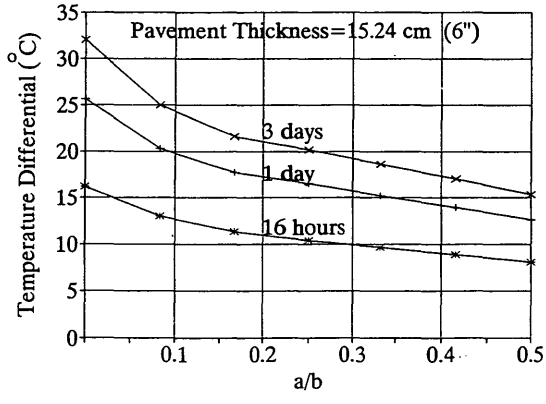

FIGURE 11 Temperature differential versus notch-depth ratio curves for concrete pavement 15.24 cm (6 in.) thick at various ages.

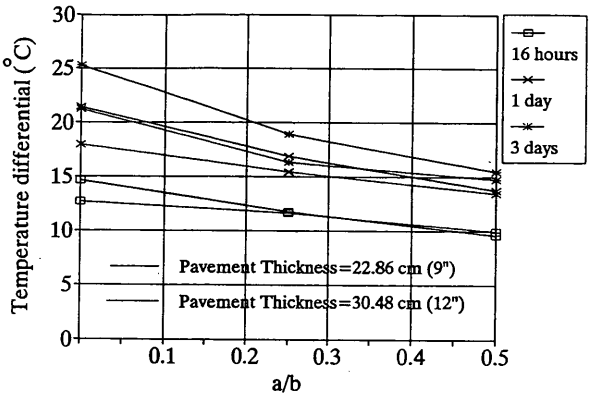

FIGURE 12 Temperature differential versus notch-depth ratio curves for concrete pavement 22.86 cm (9 in.) and 30.48 cm (12 in.) thick.

ment thickness, one can determine proper timing and optimum depth of the groove to control the formation of cracks in plain PCC pavements. Studies on the effects of shrinkage, different geometrical configurations, service loads, and concrete properties are ongoing.

CONCLUSIONS

It can be concluded from the present study that crack formation and propagation in concrete pavements can be properly analyzed using fracture mechanics. Results of crack control by introduction of a saw-cut groove are dependent on the age of the concrete, the temperature differential, and the depth of the groove. Knowing the expected temperature differential and the thickness of the pavement, one can determine the timing and groove depth that are needed to ensure proper crack control in plain concrete pavements.

It can also be concluded that timing of the saw cut is actually more important than its depth. If the saw cut is introduced after the formation of random cracking, its effectiveness in terms of crack control will be drastically reduced no matter what the depth.

REFERENCES

1. Y. S. Jenq and S. P. Shah. Feature of Mechanics of Quasi-Brittle Crack Propagation in Concrete. *International Journal of Fracture*, Vol. 51, 1991, pp. 103–120.
2. Y. S. Jenq and S. P. Shah. Two Parameter Fracture Model for Concrete. *Journal of Engineering Mechanics*, Vol. 3, No. 10, 1985, pp. 1227–1241.
3. D. S. Dugdale. Yielding of Steel Sheets Containing Slits. *Journal of the Mechanics and Physics of Solids*, Vol. 8, 1960, pp. 100–108.
4. G. I. Barenblatt. The Mathematical Theory of Equilibrium of Crack in Brittle Fracture. *Advances in Applied Mechanics*, Vol. 7, 1962, pp. 55–129.
5. A. Hillerborg, M. Modeer, and P. E. Petersson. Analysis of Crack Formation and Crack Growth in Concrete by Means of Fracture Mechanics and Finite Elements. *Cement and Concrete Research 6*, 1976, pp. 773–782.
6. J. D. Perng. *Analysis of Crack Propagation in Asphalt Concrete Using a Cohesive Crack Model*. M.S. thesis. Ohio State University, June 1989.
7. C. L. Saraf and B. F. McCullough. Controlling Longitudinal Cracking in Concrete Pavements. In *Transportation Research Record 1043*, TRB, National Research Council, Washington, D.C., 1985.
8. J. M. Armaghani, T. J. Larsen, and L. L. Smith. Temperature Response of Concrete Pavements. In *Transportation Research Record 1121*, TRB, National Research Council, Washington, D.C., 1987, pp. 23–33.
9. G. M. Jones, M. I. Darter, and G. Littlefield. Thermal Expansion-Contraction of Asphalt Concrete. *Proc., Association of Asphalt Paving Technologists*, Vol. 37, 1968, pp. 56–100.
10. RILEM Draft Recommendation: Determination of the Fracture Energy of Mortar and Concrete by Means of Three-Point Bend Tests on Notched Beams. *Materials and Structures*, Vol. 18, 1985, pp. 287–290.
11. J. M. Richardson and J. M. Armaghani. Stress Caused by Temperature Gradient in Portland Cement Concrete Pavements. In *Transportation Research Record 1121*, TRB, National Research Council, Washington, D.C., 1987, pp. 7–13.

Publication of this paper sponsored by Committee on Rigid Pavement Design.